Chitosan patterning on titanium implants

Eduardo Gilabert-Chirivella[1], Ricardo Pérez-Feito[2], Clarisse Ribeiro[3], Sylvie Ribeiro[3], Daniela M. Correia[3,4], Maria Luisa González-Martín[5,6], José María Manero[6,7,8], Senentxu Lanceros-Méndez[3], Gloria Gallego Ferrer[1,6,*], José Luis Gómez-Ribelles[1,6,*]

[1]*Centre for Biomaterials and Tissue Engineering (CBIT), Universitat Politècnica de València, Camino de Vera s/n, 46022, Valencia, Spain*

[2]*Applied Thermodynamics Department, Universitat Politècnica de València, Camino de Vera s/n. 46022, Valencia, Spain*

[3]*Centro/Departamento de Física, Universidade do Minho, Campus de Gualtar, 4710-057 Braga, Portugal*

[4]*Centro/Departamento de Química, Universidade do Minho, Campus de Gualtar, 4710-057 Braga, Portugal*

[5]*Department of Applied Physics, University of Extremadura, Avda de Elvas s/n, 06006 Badajoz, Spain*

[6]*Biomedical Research Networking Center in Bioengineering, Biomaterials and Nanomedicine (CIBER-BBN), Spain*

[7]*Biomaterials, Biomechanics and Tissue Engineering Group, Department of Materials Science and Metallurgical Engineering (UPC), ETSEIB, Av. Diagonal 647, 08028 Barcelona, Spain*

[8]*Centre for Research in NanoEngineering (CRNE) (UPC), C/Pascual i Vila 15, 08028 Barcelona, Spain*

*Corresponding authors. Tel.: +34 963877275; fax: +34 963877276.

E-mail: ggallego@ter.upv.es; jlgomez@ter.upv.es

Abstract

Titanium and its alloys are widely used in medical implants because of their excellent properties. However, bacterial infection is a frequent cause of titanium-based implant failure that also compromises its osseointegration. In this study, we report a new simple method to provide antibacterial properties to titanium surfaces by the alternation of antibacterial chitosan domains with titanium domains in the micrometric scale. Surface microgrooves were etched on pure titanium disks at intervals of 60 µm using a modified 3D printer and were then coated with the antibacterial polysaccharide chitosan. The dimensions of patterned microgrooves allowed fixing the chitosan domains to the titanium substrate without the need for covalent bonding. These domains were stable after 5 days of immersion in water and decreased the contact angle of the surfaces. Preliminary cell adhesion assays demonstrates that MC3T3-E1 pre-osteoblasts preferentially adhered to the titanium regions, while C2C12 myoblasts were uniformly distributed over the whole surface.

Keywords: Titanium, microgrooves, chitosan, myoblasts, pre-osteoblasts, cell adhesion

1. Introduction

Titanium and titanium alloys are widely used in medical devices such as dental and orthopedic implants [1] due to their excellent properties, including: chemical stability [2], low Young´s modulus [3], low thermal conductivity [4] and biocompatibility [5].

However, despite the superior properties of this material, implant failure may still occur, very often due to bacterial infection [6]. For instance, in a 15-year study Phillips *et al.* [7] reported that 0.57% of patients with a hip replacement and 0.86% with a knee replacement

developed a deep infection. In fact, many studies report the appearance of an implant infection in approximately 0.3-4% of cases [7][8][9][10].

Even though the levels of success are relatively high, unsuccessful cases involve a large number of patients, as the percentage of the population given implant surgery increases every year [9]. For example, in the UK, a total of around 40,000 hip and knee replacements are performed annually [7], while in the US in 2006 approximately 800,000 of these procedures were carried out. Economic impact of surgical site infections is quite high as the average length of hospital stays after orthopedic surgery is prolonged with an increased cost per stay of about $15,500 per patient in the US [11].

Several strategies have been proposed to modify the titanium surface to inhibit bacterial infections. Some of these include: adding inorganic molecules capable of killing bacteria to the implant surface, e.g. silver [6] or zinc [12] particles; preventing the formation of bacterial biofilm by means of cross-linked albumin coatings [13]; using the photocatalytic properties of titanium to create anti-bacterial surfaces [14] or covalent bonding of antibiotics to surfaces [15].

Also of interest is coating the titanium surface with organic, antibacterial materials such as chitosan [16], widely used in the food [17], textile [18] and medical industries [19][20]. One of the reasons for its many uses is its antibacterial properties, which act through different factors including: microorganism species, molecular weight, chelating capacity, charge density and degree of deacetylation, pH and temperature. Although several theories have been proposed to explain chitosan’s antibacterial mode of action, this is not yet clear [22]. Nevertheless, the most widely accepted view attributes the electrostatic alterations to the amine groups present in chitosan´s structure, which give it cationic characteristics. So that when chitosan comes into contact with bacterial cell walls, these

suffer large alterations, mainly in their permeability, provoking osmotic imbalances which give rise to leakage of intracellular substances (like glucose, proteins and ions), making it impossible for the bacteria to carry out their normal biological processes and causing their death [28][29][30][31].

In principle, the ideal implant should fulfill the following criteria [32]: biocompatibility, anti-infective efficiency, uncompromised fixation properties, durable anti-infective effect, good mechanical properties and stability of the antibacterial coating.

Many attempts have been made to functionalize titanium with chitosan, via: silanization [33], deposition of carboxymethyl chitosan [9], by a chitosan/hydroxyapatite composite [34], with a chitosan-lauric acid conjugate [35] or via electrodeposition [36]. These techniques involve coating the entire surface with chitosan, but as far as we know nobody has attempted to functionalize titanium surfaces with chitosan in micrometric domains. The aim of this study was therefore to develop new implant surfaces with improved antibacterial properties by accumulating chitosan in microgrooves etched into the titanium surface. The stability of the chitosan in the sample immersed in aqueous media was assessed and surface wettability (surface energy) was also explored, as it is a key factor in the biological interaction of materials. This preliminary study is an initial approach to determining how well cells adhere to this new type of surface.

2. Materials and methods

2.1. Preparation of titanium surfaces with micrometric chitosan domains

The method we developed to obtain titanium surfaces with alternated antibacterial chitosan domains consists of two steps. In the first one, parallel microgrooves were

practiced in smooth titanium surfaces and, in the second one, they were filled with chitosan.

Pure cp-titanium disks 10 mm in diameter were obtained from Technalloy (SantCugat del Valles; Spain). According to the supplier, this material contains a maximum of 0.03% nitrogen, 0.3% iron and 0.25% oxygen. They were smoothed up to a surface roughness (R_a) of under 40 nm. Once polished, the samples were cleaned with isopropanol, ethanol, water and acetone by sonication. Parallel microgrooves were etched at intervals of 60 µm by means of a novel method. For this, a G11 scalpel blade was coupled to a 3D-printer and it was set to etch parallel microgrooves on the surface of the titanium samples with the required separation through the Python programming language. The blade feed rate was set a 60 mm/min, as it provided the cleanest grooves. A circular area of 6 mm in diameter was grooved in three replicates of the titanium samples.

The samples were then placed under a nitrogen flow to remove any shavings. Next, the surface of the samples was gently rubbed with P2000 sandpaper to remove the burrs left behind after the mechanical process. The final cleaning consisted of washing the samples three times for ten minutes in an ultrasonic bath with distilled water, ethanol, and distilled water, respectively. The samples where then allowed to dry at room temperature.

After making the grooves in the titanium surfaces, they were filled with chitosan. For this, 3% w/v practical grade chitosan solution (Chitosan from crab shells. Practical grade. CAS 9012-76-4) was prepared using dilute acetic acid (3% w/v). Using a 000 nylon brush, a very small droplet (1-2 µl) of the chitosan solution was spread on the grooved titanium surface. The excess chitosan was removed from the surface by wiping 10 times in the direction of the grooves using a nylon cloth (90 µm pore size). The samples were then submerged for three hours in a 1 M sodium hydroxide solution to neutralize protonated amines from the chitosan. Finally, the samples were washed in distilled water until neutral

pH (≈7) was achieved and left to dry in a vacuum oven overnight. The samples with and without chitosan were identified as functionalized (F) and non functionalized (NF).

2.2. Microscopy

Different microscopy techniques were used to determine the actual separation and depth of the grooves. Optical microscopy was performed by an Olympus Lext OLS 3100 instrument. Scanning confocal laser microscopy by Nikon C1 microscope was used to obtain a cross-sectional view of the grooved surfaces. The stripe-like pattern of the chitosan inside the grooves of the titanium was observed with a fluorescence microscope (Nikon Eclipse 80i microscope) at an excitation of 488 nm. Field emission scanning electron microscopy (FESEM – FIB 6 Auriga Compact) was carried out to confirm the presence of chitosan inside the microgrooves of the titanium samples. Prior to observation, the samples were freeze-dried and sputter coated with platinum to ensure the conductivity of the chitosan functionalized surfaces.

To calculate the separation between the grooves, three images were taken by confocal microscopy in different zones; the distance between the grooves was calculated measuring the distance from the middle of a valley to the middle of the following valley and the mean value was calculated. The width of the microgrooves was obtained by measuring the horizontal distance halfway between the walls. The depth of the grooves was also measured. The results are expressed as the mean ± standard deviation of 25 measurements.

2.3. Water contact angle

Contact angle measurements were performed at room temperature in a Data Physics OCA 20 set-up and SCA20 software. Droplets of 2 µl of ultra pure water were dropped onto the dry surfaces. A total of three measurements were taken and an average value was used. Water contact angle was determined for functionalized (F) and non functionalized

(NF) samples and was measured parallel (//) and perpendicular (⊢) to the direction of the microgrooves at t = 0 min and t = 5 min. Values were analyzed for t = 5 min, as it was considered that after this time the drop had stabilized.

2.4. Stability of chitosan in the grooves of titanium surfaces

The stability of the chitosan inside the titanium microgrooves in immersion in water was analyzed to make sure that the chitosan would not come out of the grooves during cell culture. A chitosan functionalized titanium sample was immersed in distilled water for five days. The weight of the sample was checked before and after the test (with the sample always dry). Fluorescent microscopy was also used to determine the presence of chitosan once the experiment had concluded.

2.5. Cell culture

To sterilize the supports before cell culture, circular titanium samples functionalized and non-functionalized with chitosan lines were exposed to ultraviolet (UV) light for 1 h each side and washed 3 times in a phosphate buffer saline (PBS) solution for 5 min each wash. Two different cell lines were used: mouse C2C12 myoblast and mouse MC3T3-E1 pre-osteoblast. C2C12 and MC3T3-E1 cells were grown in 75 cm^2 cell-culture flask and cultured in Dulbecco's Modified Eagle's Medium (DMEM, Gibco) containing 4.5 $g \cdot L^{-1}$ and 1 $g \cdot L^{-1}$, respectively, supplemented both with 10 % Fetal Bovine Serum (FBS, Biochrom) and 1 % Penicillin-Streptomycin (P/S, Biochrom). Flasks were incubated at 37 ºC in humidified air containing 5% CO_2 atmosphere. The culture medium was changed every two days until confluence (60-70%) and after that they were trypsinized with 0.05 % trypsin-EDTA. Cell culture was then performed on the samples. The samples were placed in a 24-well plate and 5,000 cells were seeded in each sample for both cell types. Controls were run at the same time and same concentration in wells without material. Cell proliferation was evaluated after 2 days for both cell types.

3. Results and Discussion

3.1. Morphology of the Ti-patterned surfaces

The work involved producing a new type of surface by creating parallel microgrooves on the surface of pure titanium samples. Images obtained by optical microscopy showed neat parallel microgrooves on the surface of the titanium samples (Figure 1a). A more detailed view of the surface of the titanium in the ridges and valleys of the grooved sample can be seen in the FESEM images in Figure 1b, while a 3D reconstruction of the surface was obtained by confocal microscopy (Figure 1c) which allowed a reconstruction of the cross-section of the sample surface (a representative example is shown in Figure 1d). The combination of the three microscopy techniques allowed us to quantify the topography of the titanium substrates. The mean separation between the grooves was determined by optical microscopy. The average and standard deviation of the distance between the axis of consecutive grooves was determined to be 66.8 ± 13.7 μm. The width and depth of the grooves were determined from confocal microscopy images. The depth and width of the grooves were 17.6 ± 4.6 μm and 36.3 ± 6.0 μm respectively.

The separation between the grooves was controlled in the patterning of the sample surface using IT software (using our own algorithm in *Python* programming language), and taking into consideration that the desired separation was 60 μm, which was achieved with a fairly good degree of precision. The depth and width depended on the force applied and the shape of the etching blade. The dimensions obtained allowed (see below) fixing a chitosan coating to the grooves without the need for covalent bonding of the coating to the titanium substrate. FESEM images show that the sanding of the grooves apparently crushed the burrs on the ridges of the microgrooves, creating a micro-topography on the surface. It has been shown that the rough surfaces of titanium prostheses enhance osseointegration, although there is no agreement on the optimal degree of roughness. For

example, Song *et al*. [37] demonstrated that microgrooves with a width of 60 μm and depth of 10 μm promoted implant osseointegration (see also Junker *et al*. [38]). As the topography created could therefore provide better properties than a surface with polished ridges, no further polishing was performed.

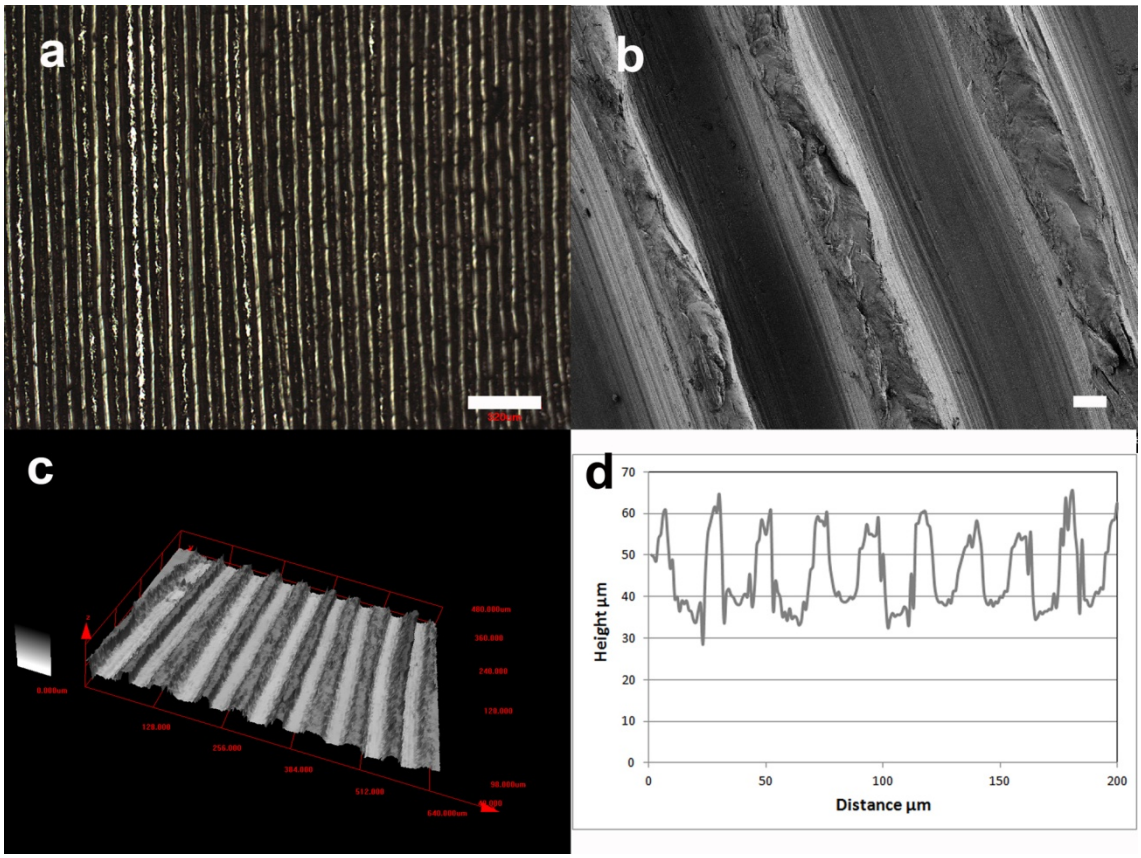

Figure 1. Microscopy images of grooved titanium substrates: (a) optical microscopy shows the parallel grooves etched in the titanium surface, (b) FESEM image in which the different topography of the ridges and the valleys can be appreciated, (c) 3D reconstruction by confocal microscopy and (d) an example of reconstructed cross-section built up from confocal microscopy images. Dimension bar corresponds to 300 μm in (a) and 10 μm in (b)

3.2. Chitosan domains within the grooves of titanium: morphology and stability

The chitosan coating was fixed to the bottom of the grooves only by physical interactions with no covalent bonding to the titanium surface. The coating only required solvent casting of chitosan from the aqueous solution, followed by cleaning the ridges of the grooves and final deprotonation of the amine groups by immersing the substrate in a

sodium hydroxide solution that yields an insoluble chitosan coating. Chitosan's self fluorescence was used to get a qualitative assessment of the presence of chitosan in the grooves. The image obtained in the fluorescence microscope just after chitosan neutralization is shown in Figure 2a. Clear fluorescent bands can be observed, together with some highly fluorescent dots, which were probably due to chitosan aggregates formed in the grooves and ridges. The appearance of some of the chitosan domains in the ridges is due to the roughness of the titanium surface caused by the grooving process in the 3D printer, followed by the sanding. This topography hinders the complete cleaning of the ridges after the chitosan solution is fixed to the surface. Obviously, more thorough polishing would improve cleaning. The substrates were immersed in water for different times to check the stability of the chitosan layer. Figure 2b shows the image obtained after 5 days of immersion. Chitosan stripes are clearly observed before and after the test. The roughness of the titanium surface inside the grooves, with a pattern of microgrooves parallel to the groove axis, helps to fix the chitosan to the surface and keep it there, even if no covalent bonds are formed between the organic and inorganic components. The quantity of the chitosan coating was determined by weighing to be 0.2 mg/cm^2. To further check the durability of the chitosan layer on the surface, the sample weight was determined before and after water immersion, finding no significant changes in the weight to within an accuracy of 0.01 mg.

FESEM images (Figure 3a) show the change in the texture at the bottom of the groves. Figure 3b shows a detail of a zone in which the chitosan coating was incomplete and in which the thickness of the coating can be observed. This thickness can be modified to some extent by changing the concentration of the chitosan solution or by repeated chitosan applications until the grooves are nearly full.

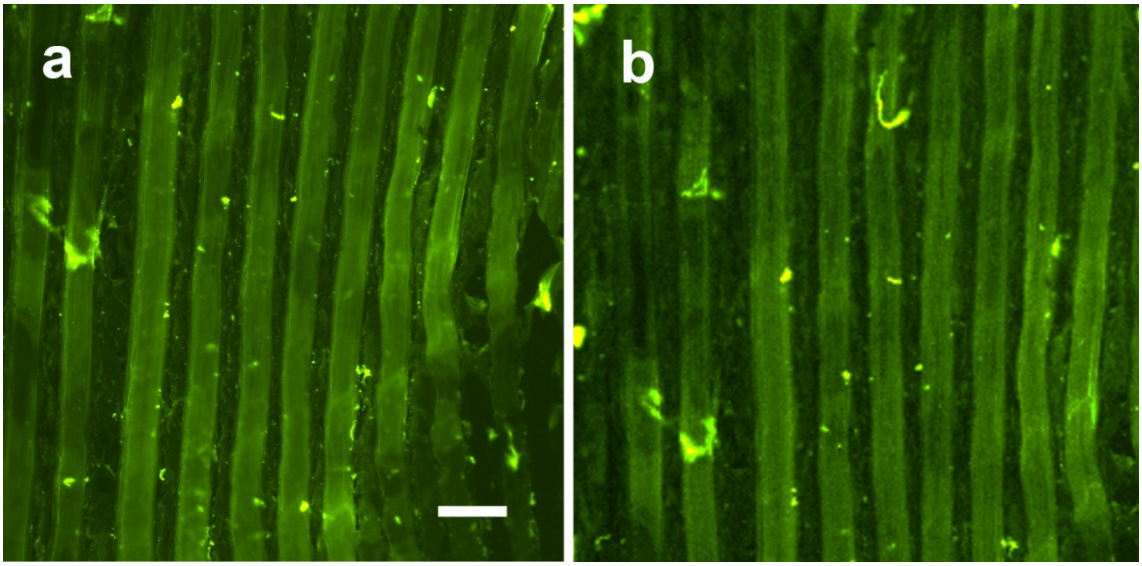

Figure 2. (a) Readily functionalized titanium sample (t = 0 days), (b) functionalized titanium sample after 5 days immersed in water (t = 5 days). The scale bar (100 μm) is valid for both images.

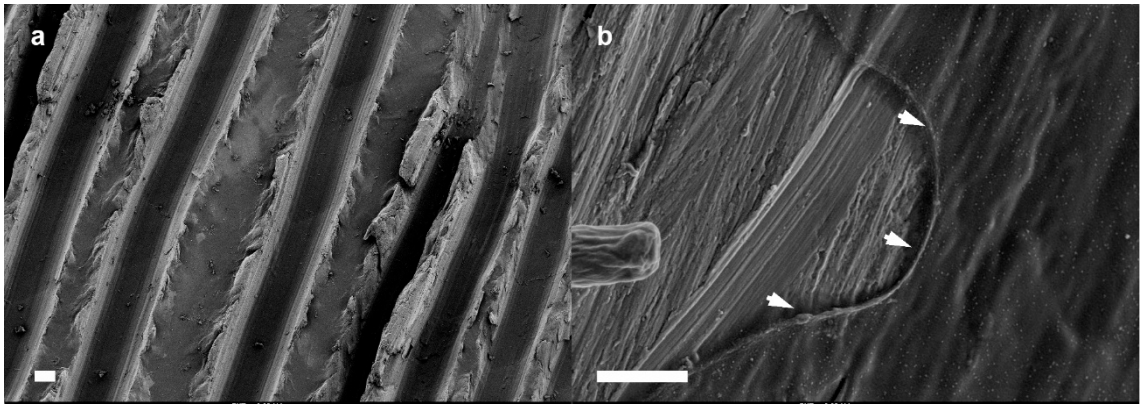

Figure 3. (a) FESEM image showing grooved titanium substrata functionalized with chitosan, (b) FESEM image showing detail of the thin chitosan coating (white arrows). Dimension bar 20 μm in (a) and 1 μm in (b)

3.3. Water contact angle

The surface patterning of hydrophilic and hydrophobic stripes is expected to yield an increase of surface wettability, with respect to either the flat or grooved titanium surface. Wettability is a clue property in cell adhesion and in the integration of the prosthetic implant in the host tissue. When the water drop is deposited on the grooved sample, it spreads to some extent in the direction of the grooves, due to capillarity, so the contact

angle measured in the direction of the grooves is always higher than that measured in the direction perpendicular to the grooves, as shown in Figure 4. The water contact angle values of the different titanium samples are shown in Figure 4. It can be seen that unfunctionalized samples are more hydrophobic than functionalized samples when measured in the same direction, due to the hydrophilicity of the chitosan coating.

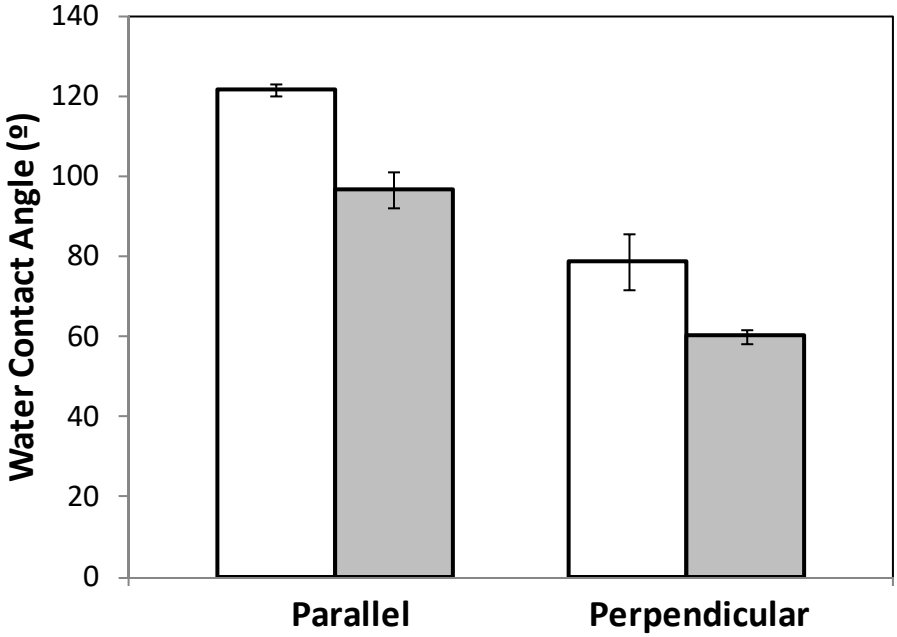

Figure 4. Water contact angle at room temperature for the functionalized (F) (grey) and non-functionalized (NF) (white) dry titanium samples. The water contact angle of droplets of 2 µl of ultra pure water deposited on the surface of the materials was measured parallel and perpendicular to the direction of microgrooves practiced in the titanium disks. Values are mean ± standard deviation.

3.4. Cell culture

A preliminary study of cell adhesion was performed on the hybrid chitosan/titanium surfaces using two different cell types to determine the different response of the different types to the hybrid surface. MC3T3-E1 is a pre-osteoblastic cell line that has been frequently used to test biomaterials aimed for bone implants or bone regeneration

scaffolds [39]. C2C12 is a myoblast cell line used for investigating muscle growth, proliferation and differentiation [40]. Both have been cultured on Ti/chitosan supports.

In this study, the cells were seeded on the substrates at the same cell density. The results after two days of cell culture can be observed in Figure 5. Cell nuclei were stained with Dapi (in blue) and the chitosan coating can be clearly observed thanks to chitosan's green autofluorescence. Interestingly, it can be seen that the cells proliferate randomly in both control samples. However, while the C2C12 myoblast cells proliferate preferentially over the chitosan lines, the MC3T3-E1 pre-osteoblast cells show higher proliferation on the titanium. Previous studies with osteoblast cells showed that a titanium coating enhanced osteoblast proliferation [41][42]. However, when the chitosan coating was placed in the titanium substrate, it was observed that the adhesion and growth of osteoblast cells were larger on the chitosan-coated samples than on the uncoated titanium [43], which disagrees with the results of the present study. No previous studies involving myoblast cells comparing chitosan with titanium have been found.

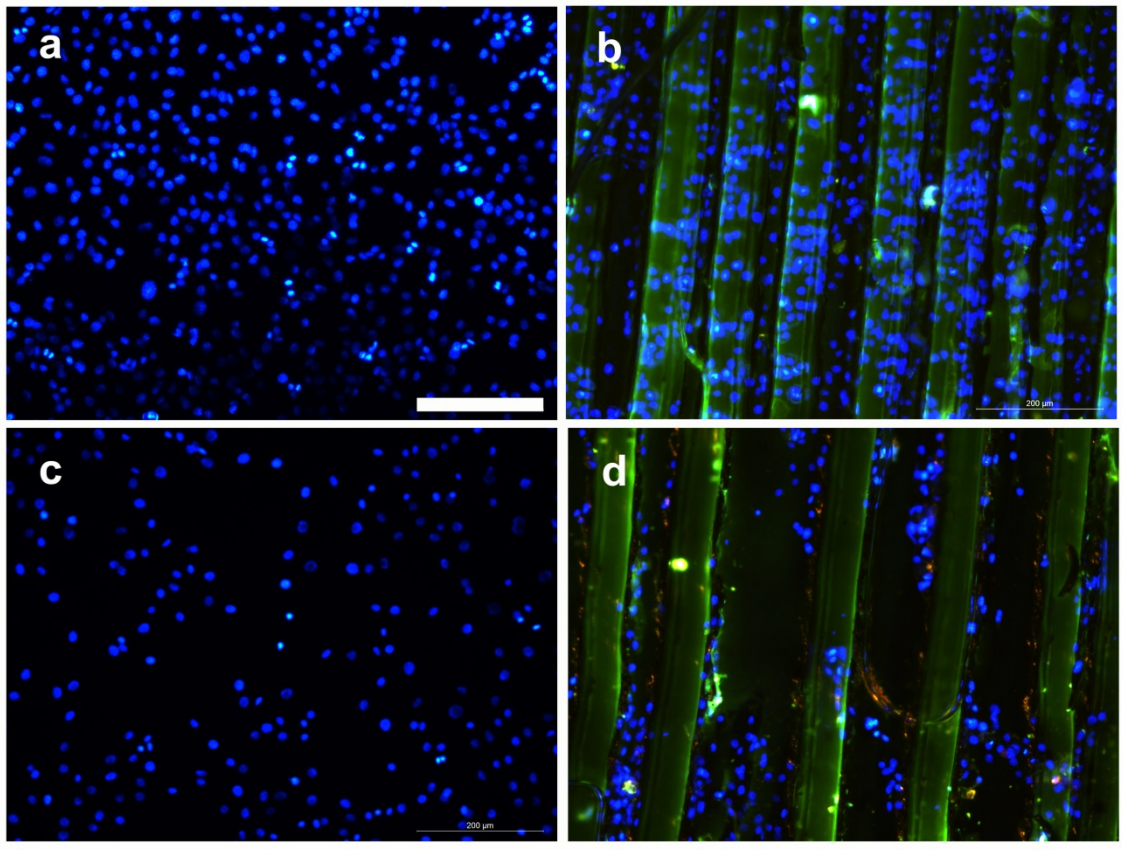

Figure 5. Immunofluorescence analysis of: C2C12 myoblast cell in (a) sample control and (b) hybrid chitosan/titanium surfaces; and of MC3T3-E1 pre-osteoblast cell in (c) sample control and (d) hybrid chitosan/titanium surfaces. Nuclei were stained blue with DAPI and the chitosan line is green. The scale bar (200 μm) is valid for all the images.

5. Conclusions

This paper describes a procedure to obtain hybrid Titanium/Chitosan surfaces with alternate strips of the organic and the metallic domains. Chitosan is deposited in the form of a thin coating on the bottom of 16 μm deep grooves. This coating is stable when the sample is immersed in water or in a culture medium, even though no covalent bonding was formed between the chitosan chains and the titanium surface. Cell adhesion to the substrates was tested with two cell lines. While myoblasts preferentially adhered to the chitosan domains, almost none of the MC3T3-E1 pre-osteoblasts were found on the chitosan, while they were seen to spread on the titanium domains.

Acknowledgments

The authors are grateful for the financial support from the Spanish Ministry of Economy and Competitiveness through the MAT2013-46467-C4-1-R Project (including Feder funds). CIBER-BBN is an initiative funded by the VI National R&D&I Plan 2008-2011, "IniciativaIngenio 2010", Consolider Program. CIBER actions are financed by the "Instituto de Salud Carlos III" with assistance from the European Regional Development Fund. CR, SR and DMC are grateful to the FCT, POPH/FSE for the SFRH/BPD/90870/2012, SFRH/BD/111478/2015 and SFRH/BD/82411/2011 grants, respectively. The authors acknowledge the assistance and advice of the Electron Microscopy Service of the UPV. We are also indebted to Dionisio García García and José García Antón of the "Instituto de Seguridad Industrial Radiofísica y Medio Ambiental" of the UPV for their assistance with the scanning confocal laser microscopy.

References

[1] X. Liu, P. K. Chu, and C. Ding, "Surface modification of titanium, titanium alloys, and related materials for biomedical applications," *Mater. Sci. Eng. R Reports*, vol. 47, no. 2004, pp. 49–121, 2004.

[2] N. Adya, M. Alam, T. Ravindranath, a Mubeen, and B. Saluja, "Corrosion in titanium dental implants: literature review," *J. Indian Prosthodont. Soc.*, vol. 5, no. 3, p. 126, 2005.

[3] M. Kulkarni, A. Mazare, P. Schmuki, and A. Iglič, "Biomaterial surface modification of titanium and titanium alloys for medical applications," *Nanomedicine*, pp. 111–136, 2014.

[4] C. L. and M. Peters, *Titanium and Titanium Alloys, Fundamentals and Applications*. 2003.

[5] L. H. Li, Y. M. Kong, H. W. Kim, Y. W. Kim, H. E. Kim, S. J. Heo, and J. Y. Koak, "Improved biological performance of Ti implants due to surface modification by micro-arc oxidation," *Biomaterials*, vol. 25, pp. 2867–2875, 2004.

[6] N. a. Trujillo, R. a. Oldinski, H. Ma, J. D. Bryers, J. D. Williams, and K. C. Popat, "Antibacterial effects of silver-doped hydroxyapatite thin films sputter deposited on titanium," *Mater. Sci. Eng. C*, vol. 32, no. 8, pp. 2135–2144, 2012.

[7] J. E. Phillips, T. P. Crane, M. Noy, T. S. J. Elliott, and R. J. Grimer, "The incidence of deep prosthetic infections in a specialist orthopaedic hospital: a 15-year prospective survey.," *J. Bone Joint Surg. Br.*, vol. 88, no. 7, pp. 943–948, 2006.

[8] L. L. D. Schwartz-Arad, A. Laviv, "Failure Causes, Timing, and Cluster Behavior: An 8-Year Study of Dental Implants," *Implant Dent.*, vol. 17, 2008.

[9] K. G. Neoh, X. Hu, D. Zheng, and E. T. Kang, “Balancing osteoblast functions and bacterial adhesion on functionalized titanium surfaces.,” *Biomaterials*, vol. 33, no. 10, pp. 2813–22, Apr. 2012.

[10] D. J. Hackett, A. C. Rothenberg, A. F. Chen, C. Gutowski, D. Jaekel, I. M. Tomek, B. S. Parsley, P. Ducheyne, and P. A. Manner, “The Economic Significance of Orthopaedic Infections,” *J. Am. Acad. Orthop. Surg.*, vol. 23, no. April, pp. 1–7, 2015.

[11] G. de Lissovoy, K. Fraeman, V. Hutchins, D. Murphy, D. Song, and B. B. Vaughn, “Surgical site infection: Incidence and impact on hospital utilization and treatment costs,” *Am. J. Infect. Control*, vol. 37, pp. 387–397, 2009.

[12] J. Fang, J. Zhao, Y. Sun, H. Ma, X. Yu, Y. Ma, Y. Ni, L. Zheng, and Y. Zhou, “Original Biocompatibility and Antibacterial Properties of Zinc-ion Implantation on Titanium,” *J. Hard Tissue Biol.*, vol. 23, pp. 35–44, 2014.

[13] Y. H. An, J. Bradley, D. L. Powers, and R. J. Friedman, “The prevention of prosthetic infection using a cross-linked albumin coating in a rabbit model.,” *J. Bone Joint Surg. Br.*, vol. 79, pp. 816–819, 1997.

[14] B. G. X. Zhang, D. E. Myers, G. G. Wallace, M. Brandt, and P. F. M. Choong, “Bioactive coatings for orthopaedic implants-recent trends in development of implant coatings,” *Int. J. Mol. Sci.*, vol. 15, pp. 11878–11921, 2014.

[15] G. Schmidmaier, M. Lucke, B. Wildemann, N. P. Haas, and M. Raschke, “Prophylaxis and treatment of implant-related infections by antibiotic-coated implants: a review,” *Injury*, vol. 37, 2006.

[16] M. Rinaudo, “Chitin and chitosan: Properties and applications,” *Prog. Polym. Sci.*, vol. 31, pp. 603–632, 2006.

[17] S. R. Kanatt, R. Chander, and A. Sharma, “Chitosan glucose complex - A novel food preservative,” *Food Chem.*, vol. 106, pp. 521–528, 2008.

[18] D. Gupta and A. Haile, “Multifunctional properties of cotton fabric treated with chitosan and carboxymethyl chitosan,” *Carbohydr. Polym.*, vol. 69, pp. 164–171, 2007.

[19] R. A. A. Muzzarelli, “Chitins and chitosans as immunoadjuvants and non-allergenic drug carriers.,” *Mar. Drugs*, vol. 8, no. 2, pp. 292–312, Jan. 2010.

[20] C. M. Deng, L. Z. He, M. Zhao, D. Yang, and Y. Liu, “Biological properties of the chitosan-gelatin sponge wound dressing,” *Carbohydr. Polym.*, vol. 69, pp. 583–589, 2007.

[21] H. K. No, N. Y. Park, S. H. Lee, H. J. Hwang, and S. P. Meyers, “Antibacterial Activities of Chitosans and Chitosan Oligomers with Different Molecular Weights on Spoilage Bacteria Isolated from Tofu,” *J. Food Sci.*, vol. 67, no. 4, pp. 1511–1514, 2002.

[22] E. I. Rabea, M. E. T. Badawy, C. V. Stevens, G. Smagghe, and W. Steurbaut, “Chitosan as antimicrobial agent: Applications and mode of action,” *Biomacromolecules*, vol. 4, no. 6, pp. 1457–1465, 2003.

[23] X. F. Liu, Y. L. Guan, D. Z. Yang, Z. Li, and K. D. Yao, “Antibacterial Action of Chitosan and Carboxymethlyated Chitosan,” *J. Appl. Polym. Sci.*, vol. 79, no. March, pp. 1324–1335, 2000.

[24] T. Takahashi, M. Imai, I. Suzuki, and J. Sawai, “Growth inhibitory effect on bacteria of chitosan membranes regulated with deacetylation degree,” *Biochem. Eng. J.*, vol. 40, pp. 485–491, 2008.

[25] T. Chung, Y. Lu, S. Wang, Y. Lin, and S. Chu, “Growth of human endothelial cells on photochemically grafted Gly – Arg – Gly – Asp (GRGD) chitosans,” *Biomaterials*, vol. 23, pp. 4803–4809, 2002.

[26] J. Li, H. Yun, Y. Gong, N. Zhao, and X. Zhang, “Investigation of MC3T3-E1 cell behavior on the surface of GRGDS-coupled chitosan,” *Biomacromolecules*, vol. 7, no. April, pp. 1112–1123, 2006.

[27] S. S. Silva, S. M. Luna, M. E. Gomes, J. Benesch, I. Pashkuleva, J. F. Mano, and R. L. Reis, “Plasma surface modification of chitosan membranes: Characterization and preliminary cell response studies,” *Macromol. Biosci.*, vol. 8, no. May, pp. 568–576, 2008.

[28] D. Raafat, K. Von Bargen, A. Haas, and H. G. Sahl, “Insights into the mode of action of chitosan as an antibacterial compound,” *Appl. Environ. Microbiol.*, vol. 74, no. 12, pp. 3764–3773, 2008.

[29] M. Kong, X. G. Chen, K. Xing, and H. J. Park, “Antimicrobial properties of chitosan and mode of action: A state of the art review,” *Int. J. Food Microbiol.*, vol. 144, no. 1, pp. 51–63, 2010.

[30] A. El Ghaouth, J. Arul, A. Asselin, and N. Benhamou, “Antifungal activity of chitosan on post-harvest pathogens: induction of morphological and cytological alterations in Rhizopus stolonifer,” *Mycol. Res.*, vol. 96, no. 9, pp. 769–779, 1992.

[31] I. M. Helander, E. L. Nurmiaho-Lassila, R. Ahvenainen, J. Rhoades, and S. Roller, “Chitosan disrupts the barrier properties of the outer membrane of Gram-negative bacteria,” *Int. J. Food Microbiol.*, vol. 71, pp. 235–244, 2001.

[32] J. Gallo, M. Holinka, and C. S. Moucha, *Antibacterial surface treatment for orthopaedic implants.*, vol. 15, no. 8. 2014.

[33] P. Renoud, B. Toury, S. Benayoun, G. Attik, and B. Grosgogeat, “Functionalization of titanium with chitosan via silanation: evaluation of biological and mechanical performances.,” *PLoS One*, vol. 7, no. 7, p. e39367, Jan. 2012.

[34] X.-Y. Ma, Y.-F. Feng, Z.-S. Ma, X. Li, J. Wang, L. Wang, and W. Lei, “The promotion of osteointegration under diabetic conditions using chitosan/hydroxyapatite composite coating on porous titanium surfaces.,” *Biomaterials*, vol. 35, no. 26, pp. 7259–70, Aug. 2014.

[35] L. Zhao, Y. Hu, D. Xu, and K. Cai, “Surface functionalization of titanium substrates with chitosan-lauric acid conjugate to enhance osteoblasts functions and inhibit bacteria adhesion.,” *Colloids Surf. B. Biointerfaces*, vol. 119, pp. 115–25, Jul. 2014.

[36] Z. Wang, X. Zhang, J. Gu, H. Yang, J. Nie, and G. Ma, “Electrodeposition of alginate/chitosan layer-by-layer composite coatings on titanium substrates.,” *Carbohydr. Polym.*, vol. 103, pp. 38–45, Mar. 2014.

[37] E. Y. Song, J. Yoon, J. Yoon, M. Lee, S. W. Lee, and N. Oh, “The effect of microgrooves on osseointegration of titanium surfaces in rabbit calvaria,” *Tissue Eng. Regen. Med.*, vol. 10, no. 6, pp. 347–352, 2013.

[38] R. Junker, A. Dimakis, M. Thoneick, and J. a. Jansen, “Effects of implant surface coatings and composition on bone integration: A systematic review,” *Clin. Oral Implants Res.*, vol. 20, no. October 2009, pp. 185–206, 2009.

[39] C. Ribeiro, V. Sencadas, D. M. Correia, and S. Lanceros-Méndez, “Piezoelectric polymers as biomaterials for tissue engineering applications,” *Colloids Surfaces B Biointerfaces*, vol. 136, pp. 46–55, 2015.

[40] P. M. Martins, S. Ribeiro, C. Ribeiro, V. Sencadas, a C. Gomes, F. M. Gama, and S. Lanceros-Mendez, “Effect of poling state and morphology of piezoelectric poly(vinylidene fluoride) membranes for skeletal muscle tissue engineering,” *RSC Adv.*, vol. 3, pp. 17938–17944, 2013.

[41] C. Ribeiro, S. Moreira, V. Correia, V. Sencadas, J. G. Rocha, F. M. Gama, J. L. Gómez Ribelles, and S. Lanceros-Méndez, “Enhanced proliferation of pre-osteoblastic cells by dynamic piezoelectric stimulation,” *RSC Adv.*, vol. 2, no. October, p. 11504, 2012.

[42] A. R. Costa-Pinto, R. L. Reis, and N. M. Neves, “Scaffolds Based Bone Tissue Engineering: The Role of Chitosan,” *Tissue Eng. Part B Rev.*, vol. 17, no. 5, pp. 331–347, 2011.

[43] J. D. Bumgardner, R. Wiser, P. D. Gerard, P. Bergin, B. Chestnutt, M. Marini, V. Ramsey, S. H. Elder, and J. A. Gilbert, “Chitosan: potential use as a bioactive coating for orthopaedic and craniofacial/dental implants,” *J. Biomater. Sci. Polym. Ed.*, vol. 14, no. 5, pp. 423–438, Jan. 2003.